Effects of Constitutive Parameters and Dynamic Tensile Loads on Radially Periodic Oscillation of Micro-Void Centered at Incompressible Hyperelastic Spheres

X.G. Yuan[1,2] **and H.W. Zhang**[1]

Abstract: The radially symmetric motion of the pre-existing micro-void centered at an incompressible hyperelastic sphere under the dynamic surface tensile loads relating to time is investigated in this paper. Some interesting conclusions are obtained by qualitatively analyzing the solutions of the motion equation of micro-void in detail; meanwhile, numerical simulations are used for understanding the obtained conclusions. In particular, it is proved that the motion of the micro-void with time would present a nonlinearly periodic oscillation if the values of the constant tensile load, the material and the structure parameters are given and that the oscillation amplitudes of the micro-void are discontinuous in some special cases; under the generalized dynamic surface tensile loads relating to time, the necessary conditions of the nonlinearly periodic oscillation of the micro-void are proposed by using the symmetric principle and the connecting rule of the phase diagrams of the differential equation that governs the motion of the pre-existing micro-void.

Keywords: Incompressible hyperelastic material; motion equation of pre-existing micro-void; dynamic load; nonlinearly periodic oscillation

1   Introduction

As is well known, products made of hyperelastic materials such as rubber and rubberlike materials are widely used in Mechanical Engineering, Petrochemical Engineering, Aeronautics and Astronautics, etc. Correspondingly, many classical problems such as finite deformation, stability and useful time of the products are worth investigating and the considerable progresses of the corresponding investigations have been made. Static deformation problems, such as inflation, bending,

---

[1] Department of Engineering Mechanics, Faculty of Vehicle Engineering and Mechanics, State Key Laboratory of Structural Analysis for Industrial Equipment, Dalian University of Technology, Dalian 116024, China. Corresponding author: zhanghw@dlut.edu.cn, yxg1971@163.com

[2] School of Science, Dalian Nationalities University, Dalian 116600, Liaoning, P.R. China

shearing, everting, straightening and stretching of the elastic stability of a spherical shell, a cylindrical tube, a thick slab, a solid sphere, etc, have been investigated by many authors by using the analytic methods, see the review articles contributed by Beatty (1987), Horgan and Polignone (1995), Attard (2003) and the monograph contributed by Fu and Ogden (2001); some numerical methods, such as shooting methods, Galerkin methods and finite element methods, are also used for studying the finite deformation problems of structures composed of hyperelastic materials, which maybe found in Hatmann (2001), Maniatty et al (2002), and so on. On the other hand, many numerical method were employed to solve the relative problems which may be found in [Atluri, et. al. (2006); Ling and Atluri (2008)]. However, for the relative dynamic problems, most of the mathematical models are described as solving the initial-boundary value problems of strong nonlinear evolution equations with time. And so they are difficult to study due to the inherent nonlinearity. At present, some classical problems have been investigated under the assumption of axisymmetric deformation, such as the radial oscillations of a cylindrical tube and a spherical shell composed of isotropic incompressible hyperelastic materials were examined by Knowles (1960, 1962); the dynamic cavitation problems were studied by Chou-Wang and Horgan (1989) for solid spheres composed of isotropic neo-Hookean materials in the context of nonlinear elastodynamics, where the outer surface of the sphere is subjected to a suddenly applied uniform radial constant tensile load; the dynamic inflation mechanisms of the motion of a hyperelastic spherical membrane were studied by Verron et al (1999); the radial oscillations of a thin cylindrical and a spherical shell were investigated by Roussos and Mason (2005) by using the Lie point symmetry structures. More investigations in the context of nonlinear elastodynamics for hyperelastic materials may be found in Dai et al (2002, 2006), Yuan and Zhang (2006), Sladek et al (2006), Rushchitsky and Simchuk (2007), Jarak et al (2007), Majorana1 and Salomoni (2008), and so on.

Interestingly, the loading forms acting on the structures are not always the constant load but the dynamic loads relating to time, such as periodic loads or step loads, etc. More recently, Yuan and Zhang (2008) presented the nonlinear dynamical analysis of a hyperelastic solid sphere composed of the transversely isotropic incompressible Valanis-Landel materials under a special class of periodic step loads. The authors proved that a cavity would form in the interior of the sphere if the surface tensile load exceeds a certain critical value and that the motion of the formed cavity with time would present a class of singular periodic oscillations; moreover, the authors also proposed the controllability conditions of finite periodic oscillations of the formed cavity under the periodic step loads.

The aim of this paper is focused on the study of the nonlinear dynamical behaviors of the pre-existing micro-void centered at a sphere composed of an incompressible

hyperelastic material under the dynamic loads relating to time, in which the loading form is a generalization that is different from the former references. In particular, we first propose the basic governing equations of the dynamic problem in the context of nonlinear elastodynamics in Subsection 2.1 and obtain the motion equation that describes the radial motion of the micro-void under the dynamic loads relating to time in Subsection 2.2. The hardcore of this paper is Section 3. In Subsection 3.1 we consider the general constant loading form. Firstly, we discuss the possible motion forms of the micro-void in terms of the constitutive and the structure parameters in detail; secondly, we conclude that the motion of the micro-void would present a nonlinearly periodic oscillation for arbitrary prescribed constant tensile loads; finally, to better understand the conclusions, we consider the transversely isotropic incompressible neo-Hookean material first contributed by Polignone and Horgan (1993) and carry out the corresponding numerical simulations. In Subsections 3.2 and 3.3 we consider the cases of the generalized periodic step loads relating to time. Interestingly, we propose all the necessary conditions of the periodic oscillation of the pre-existing micro-void by using the symmetric principle and the connecting rule of the phase diagrams of the differential equation that governs the motion of the micro-void, moreover, we also give the numerical simulations. Significantly, as the radius of the micro-void tends to zero, the conclusions on nonlinear dynamical behaviors of the micro-void obtained in this paper can describe the problems of cavity formation and motion in solid spheres approximately and reasonably.

2 Basic governing equations and solutions

2.1 Basic governing equations

For a solid sphere composed of homogeneous incompressible hyperelastic materials, where there is a pre-existing micro-void with the radius R_1 at its center. We are concerned with the radially symmetric motion of the micro-void of the sphere under dynamic surface tensile loads with different forms. Under the assumption of spherically symmetric deformation, the undeformed and the deformed configurations of the sphere are respectively given by

$$D_0 = \{(R, \Theta, \Phi) | 0 < R_1 \leq R < R_2, \ 0 < \Theta \leq 2\pi, \ 0 \leq \Phi \leq \pi\} \tag{1}$$

$$D = \{(r, \theta, \phi) | r = r(R, t) \geq 0, \ R_1 \leq R \leq R_2; \ \theta = \Theta, \ \phi = \Phi\} \tag{2}$$

where R_1 and R_2 are the radii of the inner and the outer surfaces of the undeformed structures, respectively, and $r = r(R, t)$ is the radial deformation function with time and it is to be determined.

In the absence of body force, the basic equations governing the motion of the micro-void of the sphere composed of homogeneous incompressible hyperelastic materials are as follows.

(i) Deformation gradient tensor

The deformation gradient tensor $\mathbf{F}$ associated with Eq.(2) is given by

$$\mathbf{F} = \mathrm{diag}(\lambda_r, \lambda_\theta, \lambda_\phi) = \mathrm{diag}(\partial r(R,t)/\partial t, r(R,t)/R, r(R,t)/R) \tag{3}$$

where

$$\lambda_r = \partial r(R,t)/\partial R, \ \lambda_\theta = \lambda_\phi = r(R,t)/R \tag{4}$$

are the principal values of the deformation gradient tensor $\mathbf{F}$, namely, the radial and circumference stretches.

(ii) Incompressible constraint of hyperelastic materials

The incompressible constraint of the materials requires that $\det \mathbf{F} = 1$, namely, $\lambda_r \lambda_\theta \lambda_\phi = 1$. With Eq.(4) we have

$$\frac{\partial r(R,t)}{\partial R} = \frac{R^2}{r^2(R,t)} \tag{5}$$

(iii) Constitutive equations

For incompressible hyperelastic materials, the principle components of the Cauchy stress tensor $\mathbf{T}$ is given by

$$\sigma_{rr}(r,t) = \lambda_r \frac{\partial W}{\partial \lambda_r} - p(r,t), \quad \sigma_{\theta\theta}(r,t) = \sigma_{\phi\phi}(r,t) = \lambda_\theta \frac{\partial W}{\partial \lambda_\theta} - p(r,t) \tag{6}$$

where $p(r,t)$ now represents the hydrostatic pressure with time, $W = W(\lambda_r, \lambda_\theta, \lambda_\phi)$ is the strain energy function associated with the incompressible hyperelastic materials.

(iv) Differential equation of motion

In the absence of body force, the equations of motion governing the radially symmetric motion of the sphere, i.e., $\mathrm{div}\mathbf{T}(\mathbf{x},t) = \rho_0 \mathbf{a}(\mathbf{x},t)$, reduce to the single equation

$$\frac{\partial \sigma_{rr}(r,t)}{\partial R} \left(\frac{\partial r(R,t)}{\partial R} \right)^{-1} + \frac{2}{r(R,t)} [\sigma_{rr}(r,t) - \sigma_{\theta\theta}(r,t)] = \rho_0 \frac{\partial^2 r(R,t)}{\partial t^2} \tag{7}$$

where ρ_0 is the density of the homogeneous incompressible hyperelastic materials and it is a constant.

(v) Initial-boundary conditions

Assume that the sphere in an undeformed state and at rest at time $t = 0$ satisfies

$$r(R,0) = R, \dot{r}(R,0) = 0 \tag{8}$$

Note. In this paper, it is supposed that dots over any letters denote derivatives with respect to t.

Since the outer surface of the sphere is subjected to the dynamical tensile loads $\Delta p(t)$, the surface boundary condition now requires that

$$\sigma_{rr}(r(R_2,t),t) = \Delta p(t) \left[\frac{R_2}{r(R_2,t)} \right]^2, \quad t \geq 0 \tag{9}$$

where $\Delta p(t)$ has the following forms

$$\Delta p(t) = \begin{cases} p_1, & t \in [kT, kT + t_0) \\ p_2, & t \in [kT + t_0, kT + t_0 + t_1), \\ p_3, & t \in [kT + t_0 + t_1, kT + t_0 + t_1 + t_2] \end{cases} \tag{10}$$

where $T = t_0 + t_1 + t_2$ and $k = 0, 1, 2, \cdots$, as shown in figure 1. Obviously, $\Delta p(t)$ is a periodic function with period T.

The boundary condition at the inner surface of the traction-free micro-void is given by
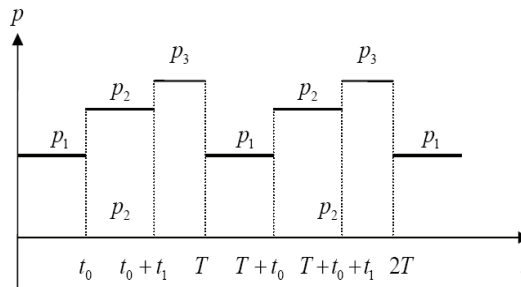
$$\sigma_{rr}(r(R_1,t),t) = 0 \tag{11}$$

Figure 1: Example forms of periodic step loads relating to time.

2.2 Solutions

On integration of Eq.(5) with respect to R yields

$$r = r(R,t) = \left[R^3 + r_1^3(t) - R_1^3\right]^{1/3}, \quad t \geq 0, \tag{12}$$

where $r_1(t)$ is the radial deformation function that describes the motion of the surface of the micro-void centered at the sphere. Interestingly, Eq.(12) implies that the motion of the radial deformation $r(R,t)$ at any points of the sphere may be completely described by $r_1(t)$. Moreover, from Eq.(12), it is not difficult to show that

$$\frac{\partial^2 r}{\partial t^2} = 2r_1 r^{-5}(r^3 - r_1^3)(\dot{r}_1)^2 + r_1^2 r^{-2} \ddot{r}_1 \tag{13}$$

Substituting Eqs.(5) and (13) into Eq.(7), and then integrating it from r_1 to r_2 with respect to r, and using the boundary conditions (9) and (11), we have

$$\Delta p(t) \left[\frac{R_2}{r(R_2,t)}\right]^2 + 2 \int_{r_1}^{r_2} \left(\lambda_r \frac{\partial W}{\partial \lambda_r} - \lambda_\theta \frac{\partial W}{\partial \lambda_\theta}\right) \frac{dr}{r}$$
$$= \rho_0 \left[\frac{1}{2} r_2^{-4} \left(r_1^4 - 4r_2^3 r_1 + 3r_2^4\right)(\dot{r}_1)^2 + r_2^{-1} r_1 (r_2 - r_1) \ddot{r}_1\right] \tag{14}$$

where $r_2 = r(R_2,t) = \left[R_2^3 + r_1^3(t) - R_1^3\right]^{1/3}$ is obtained by Eq.(12). Obviously, Eq.(14) is a second order nonlinear ordinary differential equation.

Interestingly, for the prescribed dynamical loads $\Delta p(t)$ and for different incompressible hyperelastic materials we will see that the qualitative properties of the solutions of Eq.(14) are abundant.

3   Qualitative analysis of motion of micro-void

Rewrite Eq.(12) as $R = \left[r^3 - r_1^3(t) + R_1^3\right]^{1/3}$ and introduce the following notion

$$\eta = \eta(r,r_1) = (1 - \frac{r_1^3 - R_1^3}{r^3})^{-1/3} \tag{15}$$

and so the radial and circumference stretches, i.e., Eq.(4), become $\lambda_r = \eta^{-2}$, $\lambda_\theta = \lambda_\phi = \eta$, moreover, the strain energy function can be rewritten as $\hat{W}(\eta) = W(\eta^{-2}, \eta, \eta)$. In what follows, it is convenient to introduce the following dimensionless quantities

$$x(t) = \frac{r_1(t)}{R_2}, \quad \delta = (1 - \frac{R_1^3}{R_2})^{1/3}. \tag{16}$$

From Eq.(16), it is not difficult to show that $\frac{dr}{r} = \frac{\eta^{-1}d\eta}{1-\eta^3}$. Substituting Eq.(16) into Eq. (14), we have

$$\rho_0 R_2^2 \left(x - \frac{x^2}{(\delta^3 + x^3)^{1/3}} \right) \ddot{x} + \rho_0 R_2^2 \left(\frac{x^4}{2(\delta^3 + x^3)^{4/3}} - \frac{2x}{(\delta^3 + x^3)^{1/3}} + \frac{3}{2} \right) \dot{x}^2$$
$$- \Delta p(t)(\delta^3 + x^3)^{-2/3} + h(x,\delta) = 0 \quad (17)$$

where

$$h(x,\delta) = \int_{(\delta^3+x^3)^{1/3}}^{(\frac{x^3}{1-\delta^3})^{1/3}} \frac{\hat{W}_1(\eta)}{\eta^3 - 1} d\eta \tag{18}$$

Moreover, the initial condition (8) becomes

$$x(0) = (1 - \delta^3)^{1/3}, \quad \dot{x}(0) = 0 \tag{19}$$

It is not difficult to obtain the first integral of Eq.(17), as follows,

$$A(x,\delta)\dot{x}^2 + \tilde{V}(x,\delta,\Delta p(t)) = E \tag{20}$$

where $A(x,\delta) = \frac{1}{2}\rho_0 R_2^2 x^3 \left(1 - \frac{x}{(\delta^3+x^3)^{1/3}} \right)$,

$$\tilde{V}(x,\delta,\Delta p(t)) = \begin{cases} V(x,\delta,p_1), & t \in [kT, kT+t_0) \\ V(x,\delta,p_2), & t \in [kT+t_0, kT+t_0+t_1), \\ V(x,\delta,p_3), & t \in [kT+t_0+t_1, (k+1)T] \end{cases} \tag{21}$$

$T = t_0 + t_1 + t_2, \quad k = 0, 1, 2, \cdots$ and

$$V(x,\delta,p_i) = \int_{(1-\delta^3)^{1/3}}^{x} \xi^2 h(\xi,\delta)d\xi, \quad -p_i\left((\delta^3+x^3)^{1/3} - 1\right), \; (i = 1,2,3).$$

Next we discuss the motion of the micro-void under the dynamic loading form (10) in the following cases.

3.1 Case I: $p_1 = p_2 = p_3 = P$

3.1.1 Theoretical Analysis

If it is found that $p_1 = p_2 = p_3 = P$ in Eq.(10), namely, $\Delta p(t) \equiv P$, that is to say, the sphere is subjected to a constant tensile load on its outer surface. In this case, Eq.(20) becomes

$$A(x,\delta)\dot{x}^2 + V(x,\delta,P) = E \tag{22}$$

where

$$V(x, \delta, P) = \int_{(1-\delta^3)^{1/3}}^{x} \xi^2 h(\xi, \delta) d\xi - P\left((\delta^3 + x^3)^{1/3} - 1\right) \tag{23}$$

For the initial conditions (19), we have $E = 0$, namely,

$$A(x, \delta)\dot{x}^2 + V(x, \delta, P) = 0 \tag{24}$$

It is easy to show that the implicit solution of Eq.(22) is given by

$$\pm \int_{x_0}^{x} \left(\frac{A(z, \delta)}{E - V(z, \delta, P)}\right)^{1/2} dz = t - t_0 \tag{25}$$

For the initial condition (19), Eq.(25) becomes

$$\pm \int_{(1-\delta^3)^{1/3}}^{x} \left(-\frac{A(z, \delta)}{V(z, \delta, P)}\right)^{1/2} dz = t \tag{26}$$

Obviously, for any $x > 0$ we have $A(x, \delta) > 0$, moreover, if there exists $x \in ((1 - \delta^3)^{1/3}, +\infty)$ such that the inequality $V(x, \delta, P) < 0$ is valid, we can obtain the existence conditions and the range of the real solution of Eq.(24). It can be seen that the inequality $V(x, \delta, P) < 0$ relates to not only the prescribed surface tensile load $P > 0$, but also the sphere composed of the incompressible hyperelastic materials.

On the one hand, for the strain energy function associated with the hyperelastic materials, the strongly elliptic condition, i.e., the strictly convex $d^2\hat{W}(\eta)/d\eta^2 > 0$, (c.f. Ball (1982) pp.563, Eq.(3.7)) must be satisfied, and so, if $P = 0$, we have $V_x(x, \delta, 0) > 0$ as $x \in ((1 - \delta^3)^{1/3}, +\infty)$ and $V((1 - \delta^3)^{1/3}, \delta, 0) = 0$, in other words, $V(x, \delta, 0)$ is a strictly increasing function of x. In this case, $V(x, \delta, 0) > 0$ as $x \in ((1 - \delta^3)^{1/3}, +\infty)$.

On the other hand, for any finite $P > 0$ and for any $0 < \delta < 1$, we have $V((1 - \delta^3)^{1/3}, \delta, P) = 0$ and $\lim_{x \to +\infty} V(x, \delta, P) = +\infty$. Interestingly, we can see that the function $V(x, \delta, P)$ decreases strictly with the increasing P and whether there exists a value of x such that $V(x, \delta, P) < 0$ is equivalent to $\min_{x \in (0, +\infty)} V(x, \delta, P) < 0$.

For the prescribed $P > 0$ and $0 < \delta < 1$, the critical point of $V(x, \delta, P)$ is given by the root of the equation $V_x(x, \delta, P) = 0$, namely,

$$G(x, \delta, P) = (\delta^3 + x^3)^{2/3} h(x, \delta) - P = 0 \tag{27}$$

Next we numerically study the effects of the structure parameters $0 < \delta < 1$ and the constitutive parameters on the number of solutions of Eq.(27) for the prescribed value of P.

Enlightening by the works contributed by Yuan and Zhang (2005) on the static formation of cavity and growth of a pre-existing void in incompressible hyperelastic materials, we study the relation between $P \sim x$ by starting from $\delta = 1$, namely, the solid sphere case, and so Eq.(27) becomes

$$P = (1+x^3)^{2/3}h(x,1) = (1+x^3)^{2/3} \int_{(1+x^3)^{1/3}}^{\infty} \frac{\hat{W}_1(\eta)}{\eta^3 - 1} d\eta \tag{28}$$

Obviously, the right hand of Eq.(28) is an improper integral. To insure that the value of P is finite at $x = 0^+$, we know that the following conditions on the dimensionless strain energy function $\hat{W}(\eta)$ must be valid, namely,

(i) The limit $\lim\limits_{\eta \to 1} \frac{d^2\hat{W}(\eta)}{d\eta^2}$ is a finite positive value.

(ii) The highest power of $\hat{W}(\eta)$ with respect to η does not greater than 3.

The Taylor expansion of Eq.(28) at $x = 0^+$ is given by

$$P = P_{cr} + kx^3 + o\left(x^3\right) \text{ as } x \to 0^+ \tag{29}$$

where

$$P_{cr} = \int_{1}^{\infty} \frac{\hat{W}_1(\eta)}{\eta^3 - 1} d\eta$$

and

$$k = \frac{2}{3}\left[P_{cr} - \frac{1}{6}\frac{d^2\hat{W}(\eta)}{d\eta^2}\Big|_{\eta=1}\right]$$

Eq.(29) is first obtained by Polignone and Horgan (1993) for studying static formation and growth of cavity in solid spheres composed of incompressible anisotropic nonlinearly elastic materials and P_{cr} is called the critical load that describes the critical state of cavitation in solid spheres. Moreover, it is easy to show that

$$\lim\limits_{x \to +\infty} (1+x^3)^{2/3} \int_{(1+x^3)^{1/3}}^{\infty} \frac{\hat{W}_1(\eta)}{\eta^3 - 1} d\eta = +\infty$$

by using the strongly elliptic condition of the strain energy function associated with the incompressible hyperelastic materials. In the works of Polignone and Horgan (1993), Yuan and Zhang (2005, 2006), the authors have shown that **(i)** if it is found that $k > 0$, the value of P increases from P_{cr} with respect to the increasing x from

0. See the solid line in the example curves shown in figure 3 for the transversely isotropic neo-Hookean materials. **(ii)** However, if $k < 0$, the value of P decreases locally from P_{cr} with respect to the increasing x from 0, and there must exist a secondary turning bifurcation point, written as (x_n, P_n), on the curve of $P \sim x$. See also the solid line in the example curves shown in figure 6.

However, as the values of δ are sufficiently close to 1, the solution curves of Eq.(27), i.e., $G(x, \delta, P) = 0$, are also close to those of Eq.(28). And so we will discuss the number of solutions of Eq.(27) as well as the solutions of Eq.(24) for the prescribed value of P in terms of $k > 0$ or < 0.

(i) If $k > 0$, for any prescribed $P > 0$ and for any $\delta \in (0,1)$, Eq.(27) has only one real root, see the example curves in figure 3 for different values of δ except the solid line. That is to say, $V(x, \delta, P)$ has a unique minimal point, written as $\bar{x}$, and satisfies $V(\bar{x}, \delta, P) < 0$, see the example curves in figure 4 for different values of P. Using the above analyses on the properties of $V(x, \delta, P)$, we can see that $\min\limits_{x \in (0, +\infty)} V(x, \delta, P) < 0$ is valid for any prescribed $P > 0$ and there exists a unique value of x, written as x_m, such that $V(x_m, \delta, P) = 0$. From the characteristic of Eq.(24) we know that the phase trajectories are closed and are symmetric with respect to the v-axis in the $x - v$ plane, where $v = \rho_0^{1/2} R_2 \dot{x}$. From the known theory of oscillations and the symmetric principle of ordinary differential equations we know that the solution $x(t)$ of Eq.(24) is periodic with a finite period, where the period can be obtained by Eq.(26) by setting $x = x_m$. Further, we can conclude that Eq.(24) has nonlinear periodic solutions satisfying the initial conditions (19), see the example phase diagrams in figure 5 for different values of P.

(ii) If $k < 0$, however, it can be numerically shown that there exists a value of δ, written as δ_0, such that the number of roots of Eq.(27) relating to the increasing values of P is variable. The classified discussions are as follows.

(a) If $0 < \delta \le \delta_0$, Eq.(27) has only one real root for any finite values of P, in this case, $V(x, \delta, P)$ has a unique minimal point. Similar to **(i)**, Eq.(24) has nonlinear periodic solutions satisfying the initial conditions (19) for any finite values of P.

(b) While if $\delta_0 < \delta < 1$, there exist two values of P, respectively written as P_n and P_s ($P_n < P_s$), such that the equation $G(x, P, \delta) = 0$ has only one real root if $P < P_n$ or if $P > P_s$, has two unequal real roots if $P = P_n$ or if $P = P_s$, and has three unequal real roots if $P_n < P < P_s$. See the example curves in figure 6 for different values of δ except the solid line. Relating to the information of the equation $G(x, P, \delta) = 0$, from the expression of Eq.(23) we know that $V(x, \delta, P)$ decreases strictly with the increasing values of P if $P < P_n$ and it has a unique minimal point, written as $\bar{x}_1$, moreover, the values of $\bar{x}_1$ increase with the increasing values of P; however, $V(x, \delta, P)$ has exactly two local extreme points if $P = P_n$, written as $\bar{x}_1$ and $\bar{x}_n$

($\bar{x}_1 < \bar{x}_n$), where $\bar{x}_1$ is the minimal point as above and $\bar{x}_n$ is an inflexion point. As P increases and passes through P_n and does not exceed P_s, the minimum of $V(x, \delta, P)$ taking at $\bar{x}_1$ decreases continuously with the increasing value of P, however, the inflexion point $\bar{x}_n$ splits into two local extreme points, respectively written as $\bar{x}_2$ and $\bar{x}_3$ ($\bar{x}_2 < \bar{x}_3$), in this case, $V(x, \delta, P)$ has exactly three local extreme points, written as $\bar{x}_1$, $\bar{x}_2$ and $\bar{x}_3$ ($\bar{x}_1 < \bar{x}_2 < \bar{x}_3$), moreover, $V(x, \delta, P)$ takes the local minimum at $\bar{x}_1$ and $\bar{x}_3$, and takes the local maximum at $\bar{x}_2$. Interestingly, the values of $\bar{x}_1$ and $\bar{x}_3$ increase and the values of $\bar{x}_2$ decrease with the increasing values of P as $P_n < P < P_s$, and the extreme values of $V(x, \delta, P)$ decrease correspondingly. $V(x, \delta, P)$ has exactly two local extreme points if $P = P_n$, written as $\bar{x}_s$ and $\bar{x}_3$, where $\bar{x}_s$ is another inflexion point and it is the endpoint sinked by the increasing $\bar{x}_1$ and the decreasing $\bar{x}_2$; $V(x, \delta, P)$ has exactly one minimum at $\bar{x}_3$ if $P > P_s$. See the example curves in figure 7 for different values of P. From the above analyses on the extreme points of $V(x, \delta, P)$ we know that if $k < 0$, the minimum of $V(x, \delta, P)$ is less than zero for any given tensile load $P > 0$, i.e., $\min\limits_{x \in (0, +\infty)} V(x, \delta, P) < 0$, that is to say, Eq.(24) has nonlinear periodic solutions satisfying the initial conditions (19) for any given tensile loads $P > 0$. See the example phase trajectories in figure 8 for different values of P.

Relating to the practical problems studied in this paper, we know that for any suddenly applied constant surface tensile loads P and for any given values of $0 < \delta < 1$, the motion of the initial micro-void in the interior of the sphere performs a nonlinear periodic oscillation. However, the oscillation forms are quite different for the given material parameters, structure parameters and the values of load.

Interestingly, if $k < 0$, from the qualitative properties of $V(x, \delta, P)$ we know that the phase trajectories of Eq.(24) have homoclinic orbits with the type "∞" for the given values of P satisfying $P_n < P < P_s$ and for any prescribed initial conditions, that is to say, there exactly exists a value of P, written as P_β, such that the phase trajectories of Eq.(24) starting from the initial conditions $x(0) = (1 - \delta^3)^{1/3}$ and $\dot{x}(0) = 0$ has the type "∞". Significantly, the amplitude of oscillation of the initial micro-void increases continuously with increasing surface radial tensile load satisfying $P < P_\beta$ or $P > P_\beta$. However, the amplitude of oscillation is discontinuous as P passes through P_β. See also the example phase trajectories in figure 8 for different values of P.

3.1.2 Numerical Examples

To better understand the conclusions obtained in this paper, we consider the transversely isotropic incompressible neo-Hookean material, in which the constitutive relation of the material has been discussed in detail by Polignone and Horgan

(1993). The authors also examined the static formation and growth of cavity in spheres composed of this kind of materials. The corresponding strain energy function of the transversely incompressible neo-Hookean material is given by

$$W(\lambda_1, \lambda_2, \lambda_3) = \frac{\mu}{2} \left[(\lambda_r^2 + \lambda_\theta^2 + \lambda_\phi^2 - 3) + a(\lambda_r^2 - 1)^2 \right] \qquad (30)$$

where $\mu > 0$ is the shear modulus for infinitesimal deformations, λ_i, $(i = r, \theta, \phi)$ is given by Eq.(4), and $a \geq 0$ is a parameter serves as radial anisotropy of the material. If it is found that $a = 0$, then Eq.(30) reduces to the strain energy function associated with the classical homogeneous isotropic neo-Hookean material.

Using the notations (15), we rewrite Eq.(30) as

$$\hat{W}(\eta) = W(\eta^{-2}, \eta, \eta) = \frac{\mu}{2} \left[(\eta^{-4} + 2\eta^2 - 3) + a(\eta^{-4} - 1)^2 \right] \qquad (31)$$

And so Eqs.(28) and (29) are rewritten as

$$P = 2\mu(1 + x^3)^{2/3} \int_{(1+x^3)^{1/3}}^{\infty} \frac{\eta^{-5} \left[1 - \eta^6 + 2a(\eta^{-4} - 1) \right]}{1 - \eta^3} d\eta \qquad (32)$$

$$P = 2.5 + 0.7184a + (0.3333 - 1.2989a)x^3 + o\left(x^3\right) \text{ as } x \to 0^+ \qquad (33)$$

Obviously, $k > 0$ (or < 0) in Eq.(29) is equivalent to $a < 0.2566$ (or > 0.2566) in Eq.(33) for the transversely isotropic incompressible neo-Hookean material.

The effect of the anisotropic parameter a on the growth of the micro-void of the sphere is shown in figure 2 for the given value of δ.

For the different values of the anisotropic parameter a, we present the following interesting examples.

(i) For the given value of the parameter a satisfying $a < 0.2566$ and for the different values of $0 < \delta \leq 1$, the solution curves of Eq.(27) are shown in figure 3; for the given parameters $a = 0.1$, $\delta = 0.9999$ and for the different values of P, curves of $x \sim V$ and $x \sim v$ are respectively shown in figures 4 and 5.

(ii) For the given parameters a satisfying $a > 0.2566$ and for the different values of $0 < \delta \leq 1$, the solution curves of Eq.(27) are shown in figure 6; for the given parameters $a = 1.5$, $\delta = 0.9999$ and for the different values of P, curves of $x \sim V$ and $x \sim v$ are respectively shown in figures 7 and 8.

3.2 Case II:

In this subsection, we only present the necessary conditions that the solutions of Eq.(24) satisfying the initial conditions (19) are periodic solutions under the case
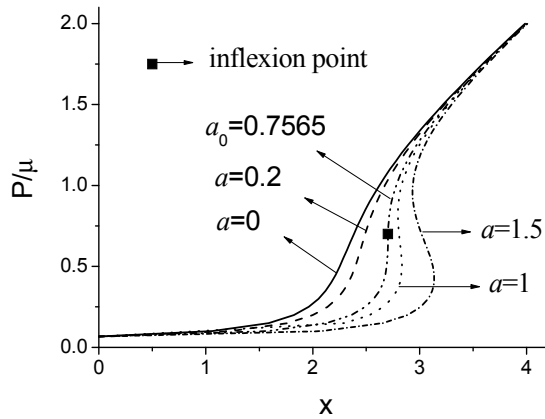
Figure 2: The effect of the anisotropic parameter a on the growth of the micro-void of the sphere as $\delta = 0.9999$.
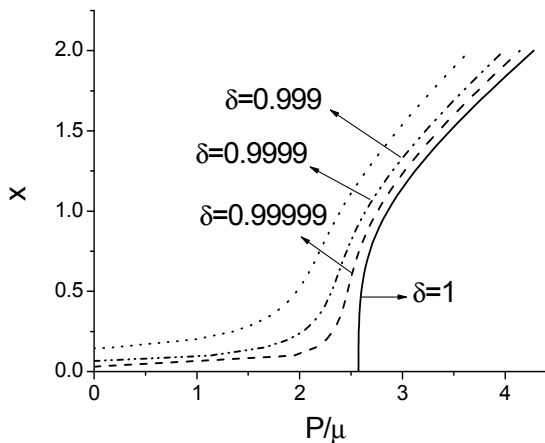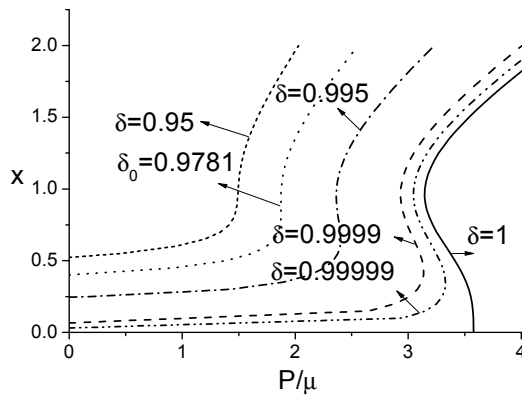

Figure 3: Effect of the structure parameter δ on the growth of the dimensionless radius x of the micro-void with the increasing P/μ for $a = 0.1$.

of , namely, the necessary conditions that the micro-void performs a nonlinear periodic oscillation under the dynamic loads relating to time. More importantly, we sufficiently use the symmetry of the phase diagrams of Eq.(24) to analyze the existence conditions of the periodic motion of the micro-void. On the other hand, to better understand the conclusions, we also consider the transversely isotropic incompressible neo-Hookean material and present the corresponding numerical figures in all cases.
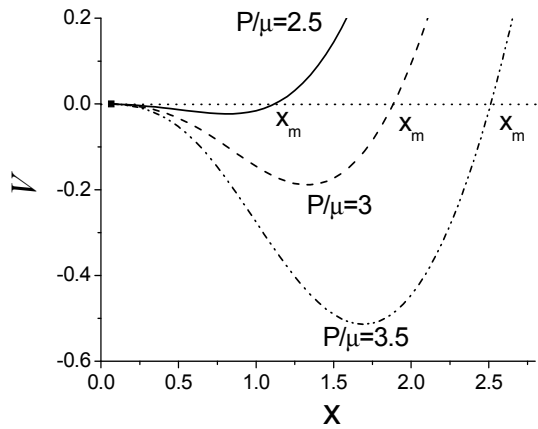
Figure 4: Curves of $x \sim V$ for $\delta = 0.9999$, $a = 0.1$ and for the different values of P/μ.
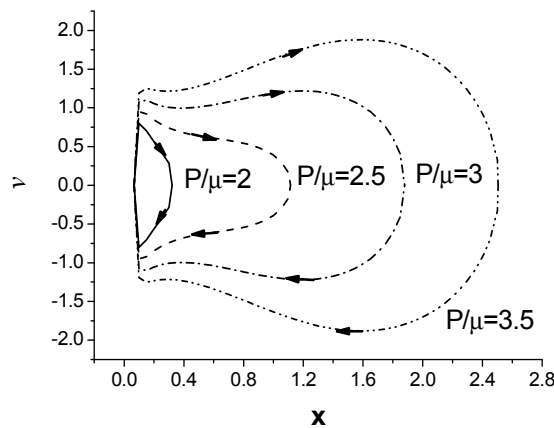
Figure 5: Phase trajectories of Eq.(24) satisfying the initial conditions (19) for $a = 0.1$, $\delta = 0.9999$ and for the different values of P/μ, where $v = \rho_0^{1/2} R_2 \dot{x}$.

(1) $t_0 = t_2$

The example forms of periodic step loading are shown in figure 9, in which the combination of the real lines means that $p_1 = p_3 < p_2$, the combination of the real lines and the dash lines means that $p_1 = p_3 > p_2$.

In what follows, we respectively denote $\hat{T}_1$ and $\hat{T}_2$ by the minimal positive periods of the oscillation of the micro-void under the different constant loads, namely, $p_1 =$

Figure 6: Effect of the structure parameter δ on the growth of the dimensionless radius x of micro-void with the increasing P/μ for $a = 1.5$.
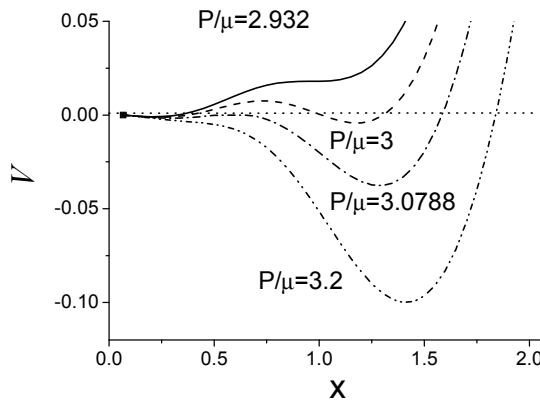

Figure 7: Curves of $x \sim V$ for $\delta = 0.9999$, $a = 1.5$ and for the different values of P/μ.

$p_3 = P$ and p_2.

(i) $t_0 = b\hat{T}_1$

Necessary conditions of periodic solutions:

$t_0 = t_2 = b\hat{T}_1$ and $t_1 = n\hat{T}_2$ (where b and n are positive integers.)

For the prescribed value of p_1, if it is found that $t_0 = b\hat{T}_1$, this means that the micro-void in the interior of the sphere oscillates periodically b times starting from $x(0) = (1 - \delta^3)^{1/3}$, $\dot{x}(0) = 0$ and ending at $x(t_0) = (1 - \delta^3)^{1/3}$ and $\dot{x}(t_0) = 0$. The tensile
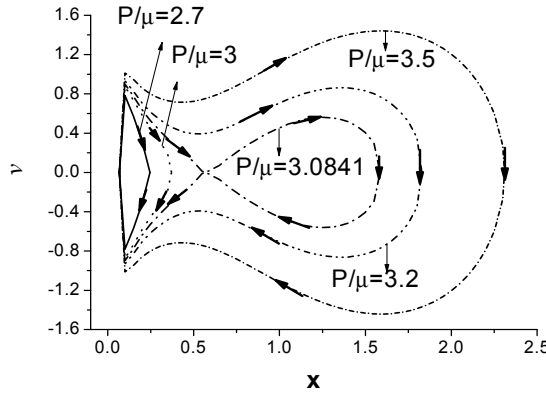
Figure 8: Phase trajectories of Eq.(24) satisfying the initial conditions (19) for $a = 1.5$, $\delta = 0.9999$ and for the different values of P/μ, where $v = \rho_0^{1/2} R_2 \dot{x}$.
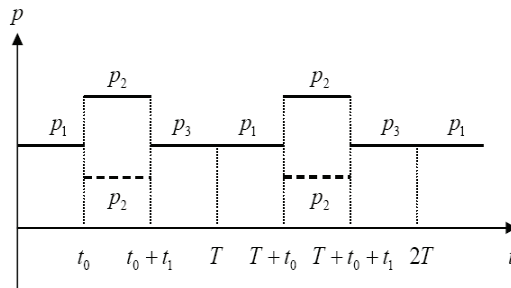

Figure 9: Example forms of periodic step loading relating to time, where $p_1 = p_3$ and $t_0 = t_2$.

load changes to p_2 in the following time. As $t \in [t_0, t_0 + t_1)$, if $t_1 = n\hat{T}_2$, namely, the micro-void oscillates periodically n times starting from $x(t_0) = (1 - \delta^3)^{1/3}$ and $\dot{x}(t_0) = 0$, moreover, $x(t_0 + t_1) = (1 - \delta^3)^{1/3}$ and $\dot{x}(t_0 + t_1) = 0$. In succession, as $t \in [t_0 + t_1, T]$, the tensile load is p_3 $(p_3 = p_1)$ and the micro-void also oscillates periodically b times. Further, in the following period T, the process will be the same as the previous process, in other words, the solutions of Eq.(24) satisfying the initial conditions (19) in this case are periodic solutions of T. Otherwise, for any values of $t_1 \neq n\hat{T}_2$, Eq.(24) has no period solutions of T. This case can be referred to the example curves shown in figures 5 and 8.

(ii) However, as $t_0 \neq b\hat{T}_1$, the motion of the micro-void will be very interesting.

(a) $t_0 = b\hat{T}_1 + \hat{T}_1/2$

Let $\hat{T}_3 = 2 \int_{\tilde{x}_0}^{x_m} \left(\frac{A(z,\delta)}{E_0 - V(z,\delta,p_2)} \right)^{1/2} dz$, where E_0 is obtained by substituting $x(t_0) = x_m$, $\dot{x}(t_0) = 0$ and the value of p_2 into Eq.(22) and $\tilde{x}_0$ is another root obtained by solving the equation $V(x,\delta,p_2) = E_0$, this means that $\hat{T}_3$ is the minimal positive period of the motion of the micro-void starting from $x(t_0) = x_m$, $\dot{x}(t_0) = 0$ and ending at $x(t_0 + \hat{T}_3) = x_m$, $\dot{x}(t_0 + \hat{T}_3) = 0$.

Necessary conditions of periodic solutions:

$t_0 = t_2 = b\hat{T}_1 + \hat{T}_1/2$ and $t_1 = j\hat{T}_3$ (where j is a positive integer.)

As $t_0 = b\hat{T}_1 + \hat{T}_1/2$, i.e., the micro-void motions from $x(0) = (1 - \delta^3)^{1/3}$, $\dot{x}(0) = 0$ and oscillates periodically b times and ends at $x(t_0) = x_m$, $\dot{x}(t_0) = 0$ at time t_0, where x_m is obtained by solving the equation $V(x,\delta,p_1) = 0$. The tensile load then changes to p_2 in the following time. If it is found that $t_1 = j\hat{T}_3$, namely, the micro-void oscillates periodically j times starting from $x(t_0) = x_m$, $\dot{x}(t_0) = 0$ and ending at $x(t_0 + t_1) = x_m$, $\dot{x}(t_0 + t_1) = 0$. As $t \in [t_0 + t_1, T]$, the tensile load is p_1 again and the radius of the micro-void reduces to the initial value $(1 - \delta^3)^{1/3}$ at time $t = 2t_0 + t_1$ and $\dot{x}(2t_0 + t_1) = 0$. This shows that the solutions of Eq.(24) satisfying the initial conditions (19) are also periodic solutions with the period T. Otherwise, as $t_1 \neq j\hat{T}_3$, along with the increasing time, the solutions of Eq.(24) will no longer be periodic solutions of T.

For the transversely isotropic incompressible neo-Hookean materials, the phase diagrams of periodic oscillation of the micro-void are shown in figures 10 ($a = 0.1$) and 11 ($a = 1.5$) as p_2 takes different values, respectively, where $t_0 = b\hat{T}_1 + \hat{T}_1/2$ and $v = \rho_0^{1/2} R_2 \dot{x}$

(b) $b\hat{T}_1 < t_0 < b\hat{T}_1 + \hat{T}_1/2$

Let $\hat{T}_4 = 2 \int_{\tilde{x}_0}^{\tilde{x}_m} \left(\frac{A(z,\delta)}{E_1 - V(z,\delta,p_2)} \right)^{1/2} dz$, where E_1 is obtained by substituting $x(t_0) = x_0$, $\dot{x}(t_0) = \dot{x}_0$ and the value of p_2 into Eq.(22), $\tilde{x}_0$ and $\tilde{x}_m$ are obtained by solving the equation $V(x,\delta,p_2) = E_1$, this means that $\hat{T}_4$ is the minimal positive period of the motion of the micro-void starting from $x(t_0) = x_0$, $\dot{x}(t_0) = \dot{x}_0$ and ending at $x(t_0 + \hat{T}_4) = x_0$, $\dot{x}(t_0 + \hat{T}_4) = \dot{x}_0$.

As $b\hat{T}_1 < t_0 < b\hat{T}_1 + \hat{T}_1/2$, this means that the motion of the micro-void starts from $x(0) = (1 - \delta^3)^{1/3}$, $\dot{x}(0) = 0$ and then the tensile load changes to p_2 as $t \in [t_0, t_0 + t_1)$, and the initial conditions that Eq.(24) satisfies are $x(t_0) = x_0$, $\dot{x}(t_0) = \dot{x}_0$ at the moment.

Necessary conditions of periodic solutions :

$b\hat{T}_1 < t_0 < b\hat{T}_1 + \hat{T}_1/2$ and $t_1 = l\hat{T}_4 + \tilde{t}$ (where l is a positive integer.)

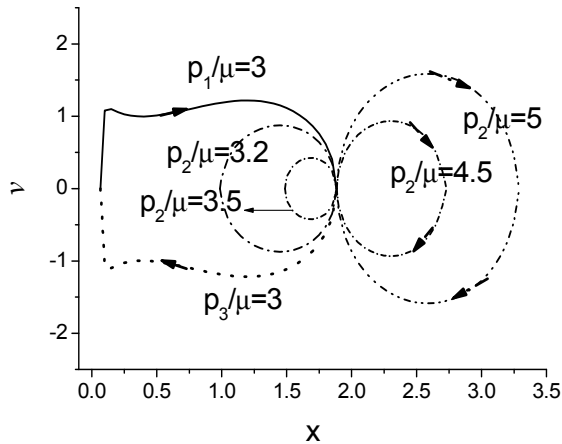If $b\hat{T}_1 < t_0 < b\hat{T}_1 + \hat{T}_1/2$, this implies that $\dot{x}_0 > 0$ (see the little pentagram in figures

Figure 10: Phase trajectories of Eq.(24) satisfying the initial conditions (19) for $a = 0.1$, $\delta = 0.9999$ and for the different values of p_2/μ.
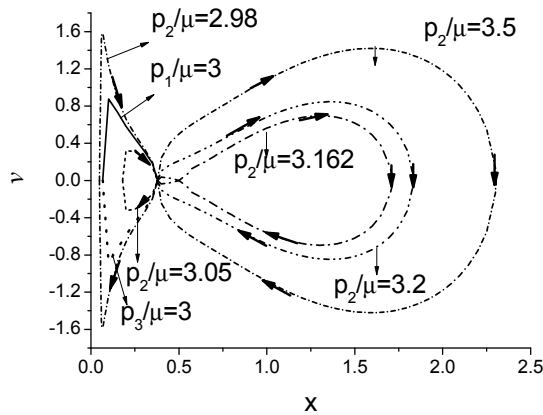

Figure 11: Phase trajectories of Eq.(24) satisfying the initial conditions (19) for $a = 1.5$, $\delta = 0.9999$ and for the different values of p_2/μ.

12 and 13), the radius of the micro-void will not increase until $\dot{x} = 0$, i.e., the cavity radius attains the local maximum, written as $\tilde{x}_m$, and the inequality $\tilde{x}_m < x_m$ (or $\tilde{x}_m > x_m$) must hold if $p_1 > p_2$ (or $p_1 < p_2$). If $t_1 = l\hat{T}_4 + \tilde{t}$ exactly, where $\tilde{t}$ is obtained by $2 \int_{x_0}^{\tilde{x}_m} \left(\frac{A(z,\delta)}{E - V(z,\delta,p_2)} \right)^{1/2} dz = \tilde{t}$, this means that the motion of the micro-void starts from $x(t_0) = x_0$, $\dot{x}(t_0) = \dot{x}_0$ and oscillates periodically l times and the values of $x(t)$ and $\dot{x}(t)$ are respectively given by x_0 and $-\dot{x}_0$ at time $t = t_0 + t_1$, namely, $x(t_0 + t_1) = x_0$, $\dot{x}(t_0 + t_1) = -\dot{x}_0$ (see the little square in figures 12 and 13).

The tensile load changes to p_1 again as $t \in [t_0 + t_1, T]$. Finally, the radius reduces to the initial value $(1 - \delta^3)^{1/3}$ at time $T = 2t_0 + t_1$ and $\dot{x}(T) = 0$. Henceforth, the motion of the micro-void will repeat as above in the following period $T = 2t_0 + t_1$. In other words, the solution of Eq.(24) satisfying the initial conditions (19) is still a periodic solution with the period T, See the example curves of phase diagrams of Eq.(24) shown in figure 12 for $a = 0.1$, $\delta = 0.9999$ and in figure 13 for $a = 1.5$, $\delta = 0.9999$. Otherwise, if $t_1 \neq l\hat{T}_4 + \tilde{t}$, along with the increasing time, the solution of Eq.(24) will no longer be a periodic solution of period T.

(c) $b\hat{T}_1 + \hat{T}_1/2 < t_0 < (b+1)\hat{T}_1$

Necessary conditions of periodic solutions:

$b\hat{T}_1 + \hat{T}_1/2 < t_0 = t_2 < (b+1)\hat{T}_1$ and $t_1 = l\hat{T}_4 + \hat{T}_4 - \tilde{t}$ (where $\hat{T}_4$ and $\tilde{t}$ are the same as those in case (b).)

If it is found that $t_0 > b\hat{T}_1 + \hat{T}_1/2$, similar to the analysis in case (b), the solution of Eq.(24) satisfying the initial conditions (19) is also a periodic solution with the period T as $t_1 = l\hat{T}_4 + \hat{T}_4 - \tilde{t}$ is hold exactly. See the example curves of phase diagrams of Eq.(24) shown in figure 12 for $a = 0.1$, $\delta = 0.9999$. That is to say, as $t \in [0, t_0)$, the micro-void oscillates b times with the initial conditions $x(0) = (1 - \delta^3)^{1/3}$ and $\dot{x}(0) = 0$ and ends at $x(t_0) = x_0$ and $\dot{x}(t_0) = \dot{x}_0$, where $\dot{x}_0 < 0$ at the moment (see the little square in figure 12); as $t \in [t_0, t_0 + t_1)$, the micro-void oscillates l times and ends at $x(t_0 + t_1) = x_0$ and $\dot{x}(t_0 + t_1) = -\dot{x}_0$ (see the little pentagram in figure 12); as $t \in [t_0 + t_1, T)$, the micro-void oscillates b times and ends at $x(T) = (1 - \delta^3)^{1/3}$ and $\dot{x}(T) = 0$. In the following period T, the micro-void will repeat the periodic oscillation. For the case of $a = 1.5$ the analyses are similar.

(2) $t_0 \neq t_2$

In this case, the tensile loading forms are slightly different from figure 9. The existence conditions of periodic solutions of Eq.(24) satisfying the initial conditions (19) are firstly given by $t_0 \neq b\hat{T}_1$ and $t_0 \neq b\hat{T}_1 + \hat{T}_1/2$. Moreover, $t_1 = l\hat{T}_4$ and $t_2 = k\hat{T}_1 + \hat{T}_1 - t_0$ must also be satisfied, where b, l and k are positive integers. Otherwise, Eq.(24) has no periodic solutions satisfying the initial conditions (19). See the example curves of phase diagrams of Eq.(24) shown in figure 12 for $a = 0.1$, $\delta = 0.9999$ and in figure 13 for $a = 1.5$, $\delta = 0.9999$.

(i) $b\hat{T}_1 < t_0 < b\hat{T}_1 + \hat{T}_1/2$,

Necessary conditions of periodic solutions:

$b\hat{T}_1 < t_0 < b\hat{T}_1 + \hat{T}_1/2$, $\quad t_1 = l\hat{T}_4$ and $t_2 = k\hat{T}_1 + \hat{T}_1 - t_0$

As shown in figures 12 and 13, the motion of the micro-void starts from the initial state $x(0) = (1 - \delta^3)^{1/3}$ and $\dot{x}(0) = 0$ under the tensile load p_1, then it oscillates b
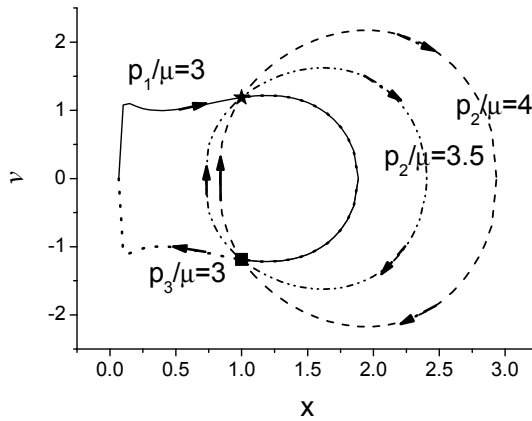
Figure 12: Phase trajectories of Eq.(24) satisfying the initial conditions (19) for $a = 0.1$, $\delta = 0.9999$ and for the different values of p_2/μ, where $t_0 \neq b\hat{T}_1 + \hat{T}_1/2$.

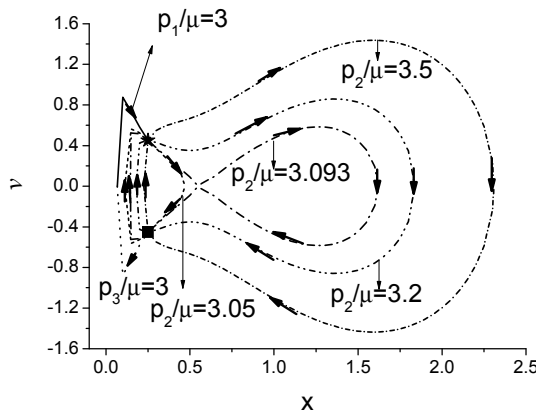
Figure 13: Phase trajectories of Eq.(24) satisfying the initial conditions (19) for $a = 1.5$, $\delta = 0.9999$ and for the different values of p_2/μ, where $t_0 \neq b\hat{T}_1 + \hat{T}_1/2$

times and reaches to the position "pentagram" at time t_0, namely, $x(t_0) = x_0, \dot{x}(t_0) = \dot{x}_0$. As $t \in [t_0, t_0 + t_1)$, the tensile load is p_2. Since $t_1 = l\hat{T}_4$, this means that the micro-void oscillates l times and ends at $x(t_0 + t_1) = x_0, \dot{x}(t_0 + t_1) = \dot{x}_0$. As $t \in [t_0 + t_1, T)$, the tensile load is p_1 again. Since $t_2 = k\hat{T}_1 + \hat{T}_1 - t_0$, this shows that the micro-void oscillates k times and ends at $x(T) = (1 - \delta^3)^{1/3}$ and $\dot{x}(T) = 0$. In the following period T, the motion will repeat again.

(ii) $b\hat{T}_1 + \hat{T}_1/2 < t_0 < (b+1)\hat{T}_1$

Necessary conditions of periodic solutions:

$b\hat{T}_1 + \hat{T}_1/2 < t_0 < (b+1)\hat{T}_1, \quad t_1 = l\hat{T}_4 \text{ and } t_2 = k\hat{T}_1 + \hat{T}_1 - t_0$

As also shown in figures 12 and 13, the micro-void oscillates b times starting from the initial state (19) and ends at the position "square" at time t_0. As $t \in [t_0, t_0 + t_1)$, the micro-void oscillates l times and ends at the position "square" at time $t_0 + t_1$ again. As $t \in [t_0 + t_1, T)$, the micro-void oscillates k times and ends at $x(T) = (1 - \delta^3)^{1/3}$ and $\dot{x}(T) = 0$. In the following period T, the motion will repeat again.

3.3 Case III: $p_1 \neq p_3$ and $p_2 \neq p_3$

(1): $t_0 = b\hat{T}_1$, $t_1 = l\hat{T}_2$ and $t_2 = k\hat{T}_5$ (where b, l and k are positive integers)

Let $\hat{T}_5$ be the minimal positive period of the oscillation of the micro-void under the constant load p_3.

In this case, Eq.(24) of course has a periodic solution satisfying the initial conditions (19) with the period T, see the example curves of phase diagrams of Eq.(24) shown in figure 5 for $a = 0.1$, $\delta = 0.9999$ and in figure 8 for $a = 1.5$, $\delta = 0.9999$. Otherwise, if one of the three conditions is not valid, the solution of Eq.(24) will not be periodic.

(2) $b\hat{T}_1 < t_0 < (b+1)\hat{T}_1$ and $t_1 \neq l\hat{T}_4$

Enlightening by the analyses in Subsection 3.2, we know that there exists a unique value of t_2 corresponding to the value of p_3 ($p_3' \leq p_3 \leq p_3''$) such that Eq.(24) has a periodic solution satisfying the initial conditions (19) with the period T for the any given $t_0 \neq b\hat{T}_1$ and $t_1 \neq l\hat{T}_4$, where p_3' and p_3'' can be obtained by . The example curves of phase diagrams of Eq.(24) in this case are shown in figure 14 for $a = 0.1$, $\delta = 0.9999$.

As shown in figure 14, the micro-void oscillates b times starting from the initial state $x(0) = (1 - \delta^3)^{1/3}$, $\dot{x}(0) = 0$ under the tensile load p_1 and ends at the position "pentagram" at time t_0. As $t \in [t_0, t_0 + t_1)$, the micro-void oscillates l times under the tensile load p_2 and ends at the position "square" at time $t_0 + t_1$ again. As $t \in [t_0 + t_1, T)$, the micro-void oscillates k times under the tensile load p_3 ($p_3' \leq p_3 \leq p_3''$) and ends at $x(T) = (1 - \delta^3)^{1/3}$ and $\dot{x}(T) = 0$. In the following period T, the motion will repeat again.

Remark. On the one hand, for spheres composed of other known incompressible hyperelastic materials, such as the modified Varga material, the Ogden material, the Valanis-landel material, the Gent-Thomas material, etc., the motion forms of the pre-existing micro-void centered at the sphere under the dynamic surface tensile loads relating to time are similar to those in this paper. On the other hand, if the loading forms are periodic loads, the motion forms of the pre-existing micro-void maybe chaotic.
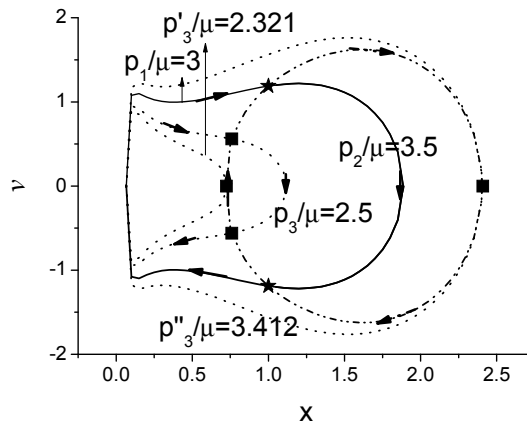
Figure 14: Phase trajectories of Eq.(24) satisfying the initial conditions (19) for $a = 0.1$, $\delta = 0.9999$ and for $t_0 \neq b\hat{T}_1$ and $t_1 \neq l\hat{T}_4$.

4 Conclusions

In this work we study the motion of the micro-void centered at an incompressible hyperelastic sphere under dynamic loads in the context of nonlinear elastodynamics and examine the effects of some parameters on the periodic oscillation forms of the micro-void by analyzing the qualitative properties of the solutions of the motion equation of micro-void in detail. The conclusions obtained in Section 3 show that the periodic oscillation forms of the micro-void not only have relation with the constitutive and the structure parameters but the dynamic loads. In particular, it is proved that the motion of the initial micro-void performs a nonlinear periodic oscillation for any prescribed constant surface tensile loads and for any prescribed material parameters, and that the periodic motions of the initial micro-void are quite different in some special cases, which may be found in Subsection 3.1. Interestingly, using the symmetric principle and the connecting rule of the phase diagrams of the motion equation of micro-void, we propose the necessary conditions of all the possible cases of nonlinearly periodic oscillation of the micro-void, which may be found in Subsections 3.2 and 3.3.

References

Attard M. M. (2003): Finite strain—-isotropic hyperelasticity. *International Journal of Solids and Structures*, Vol. 20, pp. 4353-4378.

Atluri, S. N.; Liu H. T.; Han, Z. D. (2006): Meshless local Petrov-Galerkin (MLPG) mixed finite difference Method for solid mechanics. *CMES: Computer Modeling in Engineering & Sciences*, vol.15, pp.1-16.

Ball, J. M. (1982): Discontinuous equilibrium solutions and cavitations in nonlinear elasticity. *Philos. Trans. Roy. Soc. Lond. Ser.* A, vol. 306, pp. 557-611.

Beatty, M F. (1987): Topics in finite elasticity: Hyper-elasticity of rubber, elastomers, and biological tissues–with examples. *Applied Mechanics Review*, vol. 40, pp. 1699-1733.

Chou-Wang, M-S; Horgan, C. O. (1989): Cavitation in nonlinearly elastodynamics for neo-Hookean materials. *Int J Eng Sci.*, vol.27, pp.967–973.

Dai, H. H.; Huo, Y. (2002): Asymptotically approximate model equations for nonlinear dispersive waves in incompre-ssible elastic rods. *Acta Mechanica*, vol. 157, pp. 97-112.

Dai, H. H.; Kong, D. X. (2006): Global structure stability of impact-induced tensile waves in a rubber-like material. *IMA Journal of Applied Mathematics*, vol. **71**, pp. 14–33.

Fu, Y.B.; Ogden, R.W. (2001): Nonlinear Elasticity: Theory and Applications. *Cambridge University Press*, 525 pages.

Hartmann, S. (2001): Numerical studies on the identification of the material parameters of Rivlin's hyperelasticity using tension-torsion tests. *Acta Mechanica*, vol.148, pp.1129-155.

Horgan, C. O.; Polignone, D. A. (1995): Cavitation in nonlinear elastic solids: A review. *Appl. Mech. Rev.*, vol. 48, pp. 471-485.

Jarak, T.; Soric, J.; Hoster, J. (2007): Analysis of shell deformation responses by the Meshless Local Petrov-Galerkin (MLPG) approach, *CMES: Computer Modeling in Engineering & Sciences*, vol. 18(3), pp.235-246.

Knowles, J. K. (1960): Large amplitude oscillations of a tube of incompressible elastic material. *Q Appl Math.*, vol. 18, pp. 71-77.

Knowles, J. K. (1962): On a class of oscillations in the finite deformation theory of elasticity. *J Appl Math.*, vol. 29, pp. 283-286.

Ling, X. W.; Atluri, S. N. (2008): A hyperelastic description of single wall carbon nanotubes at moderate strains and temperatures. *CMES: Computer Modeling in Engineering & Sciences*, vol.21, pp. 81-91.

Majorana1, C.E.; Salomoni, V.A. (2008): Dynamic Nonlinear Material Behaviour of Thin Shells in Finite Displacements and Rotations. *CMES: Computer Modeling in Engineering & Sciences*, vol.31, pp. 49 - 84.

Maniatty, A. M.; Liu, Y.; Klaas, O.; Shephard, M. S. (2002): Higher order stabilized finite element method for hyperelastic finite deformation. *Comput. Methods Appl. Engrg.*, vol.191, pp.1491-1503.

Polignone, D. A.; Horgan, C. O. (1993): Cavitation for incompressible nonlinearly elastic spheres. *J. Elasticity*, vol. 33, pp.27–65.

Roussos, N.; Mason D.P. (2005): Radial oscillations of this cylindrical and spherical shell. *Commu. Non. Sci. Num. Simu.*, vol. 10, pp. 139-150.

Rushchitsky, J. J.; Simchuk, Y. V. (2007): Higher-order approximations in the analysis of nonlinear cylindrical waves in a hyperelastic medium. International Applied Mechanics, Vol.43, pp.388-394.

Sladek, J.; Sladek, V.; Wen, P.H.; Aliabadi,M.H. (2006): Meshless local Petrov-Galerkiin (MLPG) method for shear deformable shells analysis, *CMES: Computer Modeling in Engineering & Sciences*, vol. 13, pp.103-117.

Verron, E.; Khayat, R. E.; Derdouri, A; Peseux, B. (1999): Dynamic inflation of hyperelastic spherical membranes. *J. Rheo.*, vol. 43, pp. 1083–1097.

Yuan, X. G.; Zhang, R. J. (2005): Effect of constitutive parameters on cavity formation and growth in a class of incompressible transversely isotropic nonlinearly elastic solid spheres, *Computers, Materials & Continua*, 2: 201-211.

Yuan, X. G.; Zhang, R. J. (2006): Nonlinear dynamical analysis in incompressible transversely isotropic nonlinearly elastic materials: Cavity formation and motion in solid spheres. *Computers, Materials & Continua*, vol. 3, pp. 119-129.

Yuan, X. G.; Zhang, H. W. (2008): Nonlinear Dynamical Analysis of Cavitation in Anisotropic Incompressible Hyperelastic Spheres under Periodic Step Loads. *CMES: Computer Modeling in Engineering & Sciences*, vol.32, pp.175-184.